

CALCULATION OF THE SCATTERING FIELDS FOR IMPEDANCE SPHERE BY USING SERIES EXPANSION METHOD

Necmi Serkan TEZEL¹ Serkan SİMSEK² Bayram ESEN³

^{1,3} Istanbul Technical University, Faculty of Electrical and Electronics Engineering
Department of Electronics and Communication Engineering,
34469, Maslak, Istanbul-Turkey

² Istanbul University, Engineering Faculty, Department of Electrical and Electronics Engineering
34850, Avcilar, Istanbul-Turkey

¹ E-mail: necmi@ehb.itu.edu.tr

² E-mail: ssimsek@istanbul.edu.tr

³ E-mail: bayram@ehb.itu.edu.tr

ABSTRACT

In this work, scattering fields of the constant impedance sphere is investigated by using series expansion of the incident and the scattering fields for different frequencies and radii of the impedance sphere. Unknown coefficients in the scattering fields are found by using impedance boundary condition. We consider the impedance sphere is illuminated by plane wave that travel along z direction. The general expressions of the scattered fields are obtained and calculated on the z=2.5 m plane (3 m x 3 m) for different frequencies and radii of the impedance sphere.

Keywords: Impedance sphere, Scattering, Impedance boundary condition

I. INTRODUCTION

Due to the appearance of non-uniform electrical structures in our environment, the scattering of electromagnetic waves by spherical bodies becomes an important issue in microwave communication systems and circuits. In the case that the relative permittivity or permeability of a scatterer is large or perfect electric conductor coated by some isolator such as paint, an approximate impedance boundary condition

(IBC) can be used to simplify the problem formulation. Impedance boundary condition which has to be satisfied on the surfaces of scattering bodies plays an important role for forward and inverse scattering problems. When impedance boundary condition is used electromagnetic waves can not penetrate to the object.

In today's technology, reduction of the radar cross section of platforms by covering them by some

Received Date : 03.01.2003

Accepted Date: 02.06.2003

proper isolator become an important topic. In this case, platform's surface can be modeled by IBC and its impedance is depended on the electromagnetic parameters of the isolator. Although the topic is important, it has not yet been thoroughly discussed in the literature because it yields extremely difficult mathematical problems. Some of the work was done about the scattering of the impedance cylinder. Mei and Van Bladel formulated the scattering of the cylinder in terms of an integral equation and then solved it numerically [1]. Later, Burnside *et al.* treated the same problem by using the geometrical theory of diffraction combined with the moment method [2]. In practice, mostly one is not interested in these works that are related to perfectly conducting bodies because these are highly idealized structures. So same problem was investigated by Erdem Topsakal, Alinur Büyükaksoy and Mithat İdemem by using Wiener Hopf equation for rectangular cylinder whose each wall has different impedance value [3]. Calculation of scattering matrix for impedance sphere was found by Necmi Serkan Tezel and Serkan Simsek [4].

The aim of this study is to consider this problem for a sphere with constant impedance using series expansion of the incident and scattering fields. In our problem, the time dependence $\exp(-i\omega t)$ will be suppressed.

The geometry of the problem is shown in Fig.1. A sphere with constant impedance is illuminated by plane wave travel along z direction. The sphere is characterized by its surface impedance Z and radius a . Because of the symmetry, it is convenient to use the scattering plane orthonormal system to express the scattering amplitudes.

In next section, the problem is first formulated as a boundary value problem. By using the series expansion of scattering fields, unknown coefficients which satisfy impedance boundary condition on the surface of the sphere is determined and then using asymptotic value of the spherical functions, bistatic radar cross-section of the object can be found.

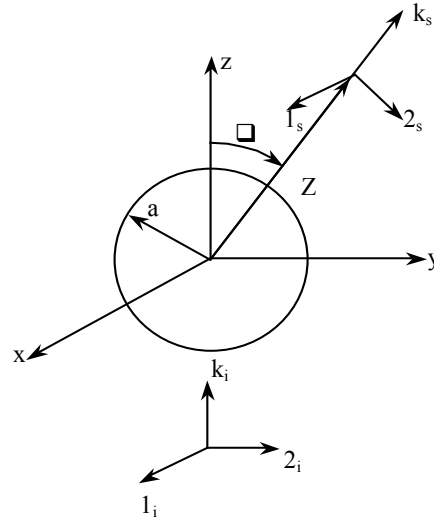


Figure 1. Geometry of the Problem

2. FORMULATION OF THE PROBLEM

Consider the impedance sphere in Fig .1. The incident plane wave has polarization \vec{e}_i and propagation direction $\vec{k}_i = \vec{e}_z$ and can be expressed by using spherical wave functions defined in [5] as,

$$\vec{E}_i = \vec{e}_i e^{jkz} = - \sum_{n=1}^{\infty} \sum_{m=-1}^{n-1} i^n \frac{(2n+1)}{n(n+1)} \left\{ \frac{\vec{e}_i \cdot \vec{C}_{-mn}(0,0)}{\gamma_{mn}} \text{Rg}[\vec{M}_{mn}(kr, \theta, \phi)] - i \frac{\vec{e}_i \cdot \vec{B}_{-mn}(0,0)}{\gamma_{mn}} \text{Rg}[\vec{N}_{mn}(kr, \theta, \phi)] \right\} \quad (1)$$

where \vec{C}_{-mn} and \vec{B}_{-mn} are spherical vector harmonics given below:

$$\vec{C}_{mn}(\theta, \phi) = \left[\vec{e}_\theta \frac{im}{\sin\theta} P_n^m(\cos\theta) - \vec{e}_\phi \frac{d}{d\theta} P_n^m(\cos\theta) \right] e^{im\phi} \quad (2)$$

$$\vec{B}_{mn}(\theta, \phi) = \vec{e}_r \times \vec{C}_{mn}(\theta, \phi) \quad (3)$$

and regular vector spherical waves, $\text{Rg}[\vec{M}_{mn}]$ and $\text{Rg}[\vec{N}_{mn}]$, are defined as

$$\text{Rg}[\vec{M}_{mn}(kr, \theta, \phi)] = \gamma_{mn} j_n(kr) \vec{C}_{mn}(\theta, \phi) \quad (4)$$

$$Rg[\vec{N}_{mn}(kr, \theta, \phi)] = \gamma_{mn} \left[\frac{n(n+1)j_n(kr)}{kr} \vec{P}_{mn}(\theta, \phi) + \frac{1}{r} \frac{\partial [rj_n(kr)]}{\partial r} \vec{B}_{mn}(\theta, \phi) \right] \quad (5)$$

$$\gamma_{mn} = \sqrt{\frac{(2n+1)(n-m)!}{4\pi n(n+1)(n+m)!}} \quad (6)$$

Here $j_n(kr)$ is spherical Bessel and $P_n^m(\cos \theta)$ is associated Legendre functions and

$$\vec{P}_{nm}(\theta, \phi) = \vec{e}_r P_n^m(\cos \theta) e^{im\phi} \quad (7)$$

To solve the boundary value problem, we let the scattered field to have the form,

$$\vec{E}_s = -\sum_{n=1}^{\infty} \sum_{m=-1,1} i^n \frac{(2n+1)}{n(n+1)} \left[-\frac{\vec{e}_i \cdot \vec{C}_{-mn}(0,0)}{\gamma_{mn}} b_n \vec{M}_{mn}(kr, \theta, \phi) + i \frac{\vec{e}_i \cdot \vec{B}_{-mn}(0,0)}{\gamma_{mn}} a_n \vec{N}_{mn}(kr, \theta, \phi) \right] \quad (8)$$

The vector spherical waves \vec{M}_{mn} and \vec{N}_{mn} are the same of $Rg[\vec{M}_{mn}]$ and $Rg[\vec{N}_{mn}]$, except Bessel function is replaced by Hankel function of the first kind.

The IBC is satisfied on the surface of the sphere ($r = a$). IBC is defined [6] as;

$$\vec{e}_r \times (\vec{E} - i \frac{Z}{k\eta} \frac{\partial \vec{E}}{\partial r}) = 0 \quad (9)$$

where

$$\vec{E} = \vec{E}^s + \vec{E}^i \quad (10)$$

substituting (10) into (9), one gets,

$$\vec{e}_r \times (\vec{E}^s - i \frac{Z}{k\eta} \frac{\partial \vec{E}^s}{\partial r}) = -\vec{e}_r \times (\vec{E}^i - i \frac{Z}{k\eta} \frac{\partial \vec{E}^i}{\partial r}) \quad (11)$$

plugging (1) and (8) into (11) gives an equation with unknown coefficients a_n and b_n . These coefficients are then solved by equating the known terms of the spherical harmonics in the right hand and left hand side of equation (11). After some mathematical operations,

$$a_n = \frac{\frac{1}{a} \frac{d[rj_n(kr)]}{dr} - i \frac{Z}{k\eta} \frac{d}{dr} \left\{ \frac{1}{r} \frac{d[rj_n(kr)]}{dr} \right\}}{\frac{1}{a} \frac{d[rh_n^{(1)}(kr)]}{dr} - i \frac{Z}{k\eta} \frac{d}{dr} \left\{ \frac{1}{r} \frac{d[rh_n^{(1)}(kr)]}{dr} \right\}} \Bigg|_{r=a} \quad (12)$$

and

$$b_n = \frac{j_n(kr) - i \frac{Z}{k\eta} \frac{d[j_n(kr)]}{dr}}{h_n^{(1)}(kr) - i \frac{Z}{k\eta} \frac{d[h_n^{(1)}(kr)]}{dr}} \Bigg|_{r=a} \quad (13)$$

are found. When one substitutes the derivatives of Bessel and Hankel functions in (12) and (13), a_n and b_n are obtained as

$$a_n = \frac{T_1 - i \frac{Z}{k\eta} T_2}{T_3 - i \frac{Z}{k\eta} T_4} \quad (14)$$

$$b_n = \frac{a J_{n+\frac{1}{2}}(ka) - i \frac{Z}{k\eta} \left[n J_{n+\frac{1}{2}}(ka) - ka J_{n+1}(ka) \right]}{a H_{n+\frac{1}{2}}^1(ka) - i \frac{Z}{k\eta} \left[n H_{n+\frac{1}{2}}^1(ka) - ka H_{n+1}(ka) \right]} \quad (15)$$

where

$$T_1 = a \left[ka J_{n-\frac{1}{2}}(ka) - n J_{n+\frac{1}{2}}(ka) \right]$$

$$T_2 = \left(n - \frac{k+1}{2} \right) a J_{n-\frac{1}{2}}(ka) + n(1-n) J_{n+\frac{1}{2}}(ka) - ka^2 J_n(ka) + nka J_{n+1}(ka)$$

$$T_3 = a \left[ka H_{n-\frac{1}{2}}^1(ka) - n H_{n+\frac{1}{2}}^1(ka) \right]$$

$$T_4 = \left(n - \frac{k+1}{2} \right) a H_{n-\frac{1}{2}}^1(ka) + n(1-n) H_{n+\frac{1}{2}}^1(ka) - ka^2 H_n^1(ka) + nka H_{n+1}^1(ka)$$

Total scattered field is expressed in terms of a_n and b_n as:

$$\begin{aligned}
 E_s = & -i \frac{e^{ikr}}{2kr} \sum \frac{(2n+1)}{n(n+1)} \\
 & \times \left[-a_n [\bar{e}_i \cdot (\bar{x} - i\bar{y})] [\bar{\theta} \tau_n(\cos \theta) + \bar{\phi} i \pi_n(\cos \theta)] e^{i\phi} \right. \\
 & - a_n [\bar{e}_i \cdot (\bar{x} + i\bar{y})] [\bar{\theta} \tau_n(\cos \theta) - \bar{\phi} i \pi_n(\cos \theta)] e^{-i\phi} \quad (16) \\
 & + i b_n [\bar{e}_i \cdot (\bar{x} - i\bar{y})] [\bar{\theta} i \pi_n(\cos \theta) - \bar{\phi} \tau_n(\cos \theta)] e^{i\phi} \\
 & \left. + i b_n [\bar{e}_i \cdot (\bar{x} + i\bar{y})] [\bar{\theta} i \pi_n(\cos \theta) + \bar{\phi} \tau_n(\cos \theta)] e^{-i\phi} \right]
 \end{aligned}$$

$\pi_n(\cos \theta)$ and $\tau_n(\cos \theta)$ are related to associated Legendre functions and defined as

$$\pi_n(\cos \theta) = -P_n^1(\cos \theta) \quad (17)$$

$$\tau_n(\cos \theta) = -\frac{dP_n^1(\cos \theta)}{d\theta} \quad (18)$$

We assume x-polarization of incident wave, then the co-polarized (x component) and cross-polarized (y component) of the scattered fields are found as

$$\begin{aligned}
 E_x^s = & i \frac{e^{ikr}}{kr} \sum_{n=1}^{\infty} \frac{(2n+1)}{n(n+1)} \{ \cos \theta \cos^2 \phi [a_n \tau_n(\cos \theta) + b_n \pi_n(\cos \theta)] \\
 & + \sin^2 \phi [a_n \pi_n(\cos \theta) + b_n \tau_n(\cos \theta)] \} \quad (19)
 \end{aligned}$$

$$\begin{aligned}
 E_y^s = & i \frac{e^{ikr}}{kr} \sum_{n=1}^{\infty} \frac{(2n+1)}{n(n+1)} \\
 & \{ \cos \theta \cos \phi \sin \phi [a_n \tau_n(\cos \theta) + b_n \pi_n(\cos \theta)] \\
 & - \sin \phi \cos \phi [a_n \pi_n(\cos \theta) + b_n \tau_n(\cos \theta)] \} \quad (20)
 \end{aligned}$$

3. NUMERICAL RESULTS

All of the numerical results are obtained for $Z=50+i50$ and $z=2.5$ m plane (3 m x 3 m). It is assumed that the magnitude of incident electric field plane wave is 1 (mV/m).

In Figs 2, 3, and 4 ; $|E_x^s|$, the magnitude of co-polarized scattered electric field is plotted for frequencies $f=100$ MHz, for three different radii.

In Figs 5, 6, and 7 ; $|E_x^s|$, the magnitude of co-polarized scattered electric field is plotted for frequencies $f=1$ GHz, for three different radii.

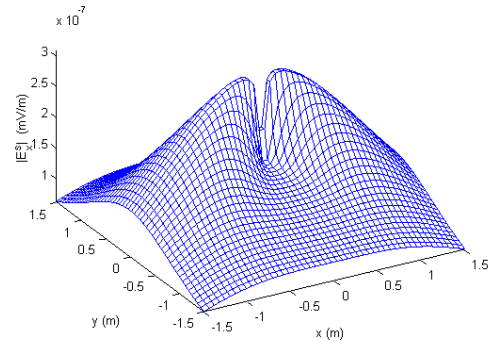


Figure 2. The magnitude of the co-polarized scattered field for $f=100$ MHz and $a=5$ cm.

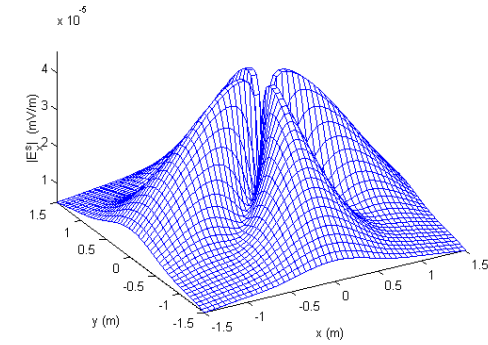


Figure 3. The magnitude of the co-polarized scattered field for $f=100$ MHz and $a=15$ cm.

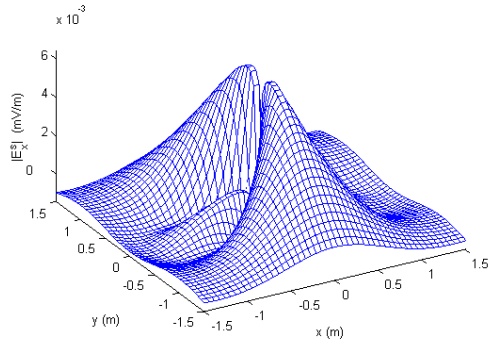


Figure 4. The magnitude of the co-polarized scattered field for $f=100$ MHz and $a=40$ cm.

In Figs 8, 9, and 10 ; $|E_y^s|$, the magnitude of cross-polarized scattered electric field is plotted for frequencies $f=100$ MHz, for three different radii.

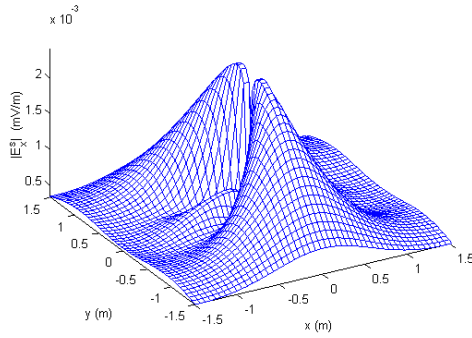


Figure 5. The magnitude of the co-polarized scattered field for $f=1$ GHz and $a=5$ cm.

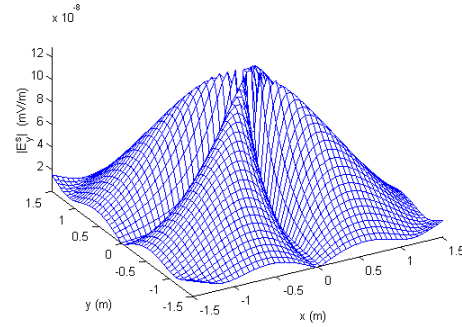


Figure 8. The magnitude of the cross-polarized scattered field for $f=100$ MHz and $a=5$ cm.

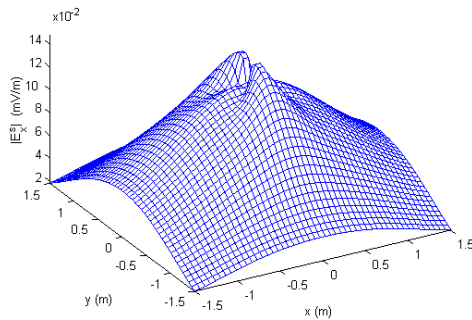


Figure 6. The magnitude of the co-polarized scattered field for $f=1$ GHz and $a=15$ cm.

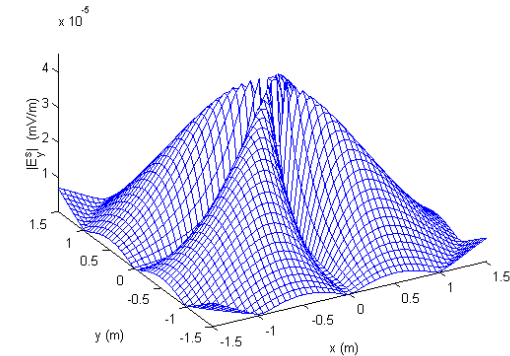


Figure 9. The magnitude of the cross-polarized scattered field for $f=100$ MHz and $a=15$ cm.

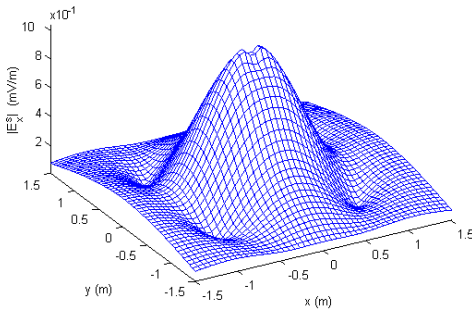


Figure 7. The magnitude of the co-polarized scattered field for $f=1$ GHz and $a=40$ cm.

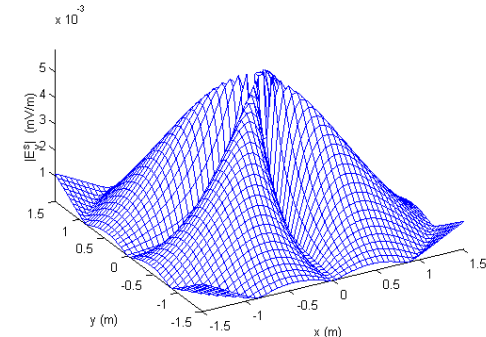


Figure 10. The magnitude of the cross-polarized scattered field for $f=100$ MHz and $a=40$ cm.

In Figs 11,12, and 13 ; $|E_y^s|$, the magnitude of cross-polarized scattered electric field is plotted for frequencies $f=1$ GHz, for three different radii.

4. CONCLUSIONS

It is observed that the magnitude of the co-polarized scattered electric field has a local maximum at the origin, $(x = 0, y = 0)$. The magnitude of cross-polarized electric field has four maxima which take place on the lines $y = \mp x$. In addition, these maxima are

symmetrical with respect to the axes Ox and Oy .

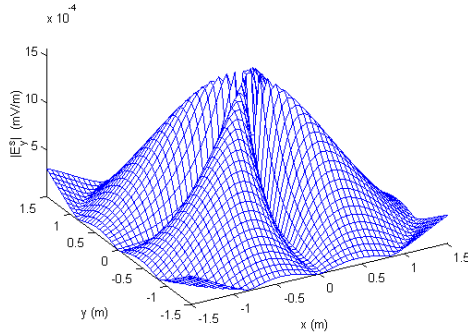


Figure 11. The magnitude of the cross-polarized scattered field for $f=1$ GHz and $a=5$ cm.

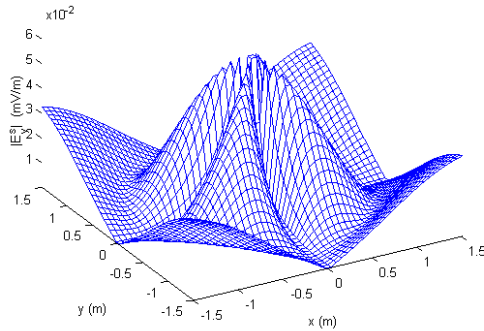


Figure 12. The magnitude of the cross-polarized scattered field for $f=1$ GHz and $a=15$ cm.

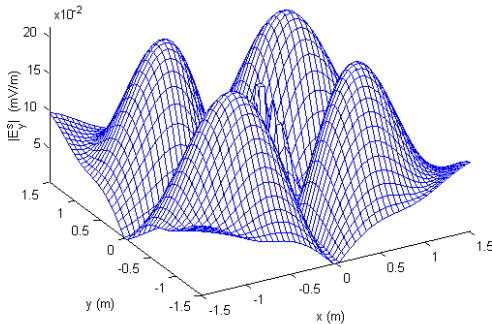


Figure 13. The magnitude of the cross-polarized scattered field for $f=1$ GHz and $a=40$ cm.

In table 1, the maximum values of the magnitude of the cross-polarized electric fields for the frequencies and radii mentioned above are tabulated. It is determined that the bigger radius correspond to the higher magnitudes.

Table I. Maximum values of the magnitude of the cross-polarized electric fields ($\mu\text{V/m}$).

radius	a=5 cm	a=15 cm	a=40 cm
frequency			
$f=100$ MHz	$13 \cdot 10^{-5}$	$45 \cdot 10^{-3}$	5.75
$f=1$ GHz	1.6	62.5	125

5. REFERENCES

[1] Mei K.K., Van Bladel J.G., "Scattering by perfectly conducting rectangular cylinders", *IEEE Transaction on Antennas and Propagation*, AP-11, (1963) pp. 185-192, 1963.

[2] Burnside W.D., Yu C.L., Marhefka R.J., "A technique to combine the geometrical theory of diffraction and the moment method", *IEEE Transaction on Antennas and Propagation*, AP-23, pp. 551-558, 1975.

[3] Topsakal E., Büyükkaksoy A., İdemem M., "Scattering of electromagnetic waves by a rectangular impedance cylinder", *Wave Motion*, pp. 273-296., 2000.

[4] Tezel N. S., Şimşek S., "Evaluation of the Scattering Matrix for Impedance Sphere", *IEEE International Symposium on Electromagnetic Compability, Istanbul, Turkey, 2003*.

[5] Tsang L., Kong J.A., Ding K.H., "Scattering of Electromagnetic Waves", John Wiley & Sons Inc., pp. 32-41, 2000.

[6] T.B.A. Senio. and J.L. Volakis, "Approximate boundary conditions in electromagnetics", *The Institution of Electrical Engineers*, 1995.



Necmi Serkan Tezel was born in Edremit, Turkey in 1978. He received the B.Sc. and M.Sc. degrees from the Istanbul Technical University Department of Electronics and Communication Engineering in 1999 and 2001 respectively. Since 1999 he has been working as a research assistant in Istanbul Technical University Department of Electronics and Communication Engineering, Division of Electromagnetic Fields and Microwave Techniques where he continues to work on his Ph.D. dissertation. His current research interests are electromagnetic theory, antennas, radar and signal processing.



Serkan Simsek was born in Amasya, Turkey in 1979. He received the B.Sc. degree from the Istanbul University Department of Electrical and Electronics Engineering in 2001 with the best degree. He continues M.Sc. degree in the Istanbul Technical University, Department of Electronics and Communication Engineering. Since 2001 he has been working as a research assistant in Istanbul University, Engineering Faculty, Department of Electrical and Electronics Engineering, Division of Electromagnetic Fields and Microwave Techniques. His current research interests are electromagnetic theory and antennas.



Bayram Esen was born in Mardin, Turkey in 1966. He received B.Sc. and M.Sc. degrees from Uludağ University, Department of Electronics and Communication Engineering in 1989 and 1992 respectively. After working as a Fellow in Kocaeli University for one year, he started a second M.Sc. degree in Texas Tech University, Department of Electrical Engineering in 1994. He graduated in August 1996. He submitted and defended a Ph.D dissertation in Istanbul Technical University, Department of Electrical-Electronics Engineering, in April 2003. He is currently working as a research assistant in İstanbul Technical University. His current research interests are electromagnetic theory and antennas.